



A Robust Image Encryption Scheme Based on Block Compressive Sensing and Wavelet Transform

Qutaiba K Abed

Informatics Institute for Postgraduate Studies
 Iraqi Commission for Computers and Informatics
 Baghdad, Iraq
 Email: phd202130682@iips.icci.edu.iq

Waleed A Mahmoud Al-Jawher

Department of Electronics and Communication Engineering
 Uruk University
 Baghdad, Iraq

Submitted: 30/11/2022. Revised edition: 31/3/2023. Accepted: 31/3/2023. Published online: 13/9/2023
 DOI: <https://doi.org/10.11113/ijic.v13n1-2.413>

Abstract—In this paper, a modified robust image encryption scheme is developed by combining block compressive sensing (BCS) and Wavelet Transform. It was achieved with a balanced performance of security, compression, robustness and running efficiency. First, the plain image is divided equally and sparsely represented in discrete wavelet transform (DWT) domain, and the coefficient vectors are confused using the coefficient random permutation strategy and encrypted into a secret image by compressive sensing. In pursuit of superior security, the hyper-chaotic Lorenz system is utilized to generate the updated secret code streams for encryption and embedding with assistance from the counter mode. This scheme is suitable for processing the medium and large images in parallel. Additionally, it exhibits superior robustness and efficiency compared with existing related schemes. Simulation results and comprehensive performance analyses are presented to demonstrate the effectiveness, secrecy and robustness of the proposed scheme. The compressive encryption model using BCS with Walsh transform as sensing matrix and WAM chaos system, the scrambling technique and diffusion succeeded in enhancement of secure performance.

Keywords—Compressive Sensing, wavelet transform, hyper-chaotic Lorenz system, Image encryption algorithm

I. INTRODUCTION

The development of several methods of transmitting information over the Internet has led to the creation of rapid techniques for transmitting digital images. This requires the secure transmission of these information's by adopting modern methods based on computer vision, such as medical vision [1-3]. Thus, encryption methods and algorithms have varied to deal with such high amounts of data as Data Encryption Standard (DES) and Advanced Encryption Standard (AES), not suitable for image encryption scenarios [1-7].

According to the in-depth study of chaos theory, and based on its unique properties, chaotic maps have been explored, such as pseudo randomness, eroticism, non-periodicity, and high sensitivity to initial values. These properties that make the image clutter-based have led to the emergence of encryption algorithms capable of protecting image data. Based on this, cryptographic algorithms based on chaotic systems have been studied extensively [8-11]. In some of them, an image coding algorithm based on the random shift of the integer cycle and the logistic map has been proposed. In another, a dynamic image coding algorithm has been proposed based on variable-length secret key and modified Henon map. Among them, an encryption algorithm based on artificial neural networks for long-term memory was used etc.

Finally, an advanced framework has been developed based on the compression sampling (CS) techniques for down sampling and compressive. It builds on the pioneering work of Candes *et al.* [12] and Donoho [13], have demonstrated that under certain conditions, the signal can be accurately reconfigured from only a small set of measurements. This principle offers the potential to greatly reduce sampling dependence, power consumption and computation complexity in digital data acquisition applications. Due to its great practical potential, it has made great achievements in academia and industries in the past few years [14-16].

In this paper, under sampling is proposed to obtain a fast CS of natural images where the original image is divided into small blocks and each block is sampled independently. Wavelet transform is used in the CS block that gives the huge success and widely spread encryption system [17]. The main steps included in this proposal included the following: (1) A compression and encryption mechanism is designed using BCS; (2) The initial values for translation are obtained, and are used as keys throughout the algorithm; (3) The image is coded by Wavelet

transform, and the pixels of the image are then mixed. Scramble mode before CS helps to mess across the whole picture. (4) The image is divided into blocks, and then BCS is adopted. To reduce the data stored in the storage space, stored offset, rotated, measurement matrix formed the chaotic sequence and random recipes blocks are used.

II. COMPRESSED SENSING

It is a signal processing technique used to efficiently acquire and reconstruct a signal from a reduced set of measurements by using priory knowledge of the signal’s sparsity on some basis. Sparsity; as it relates to signal processing is a measure of the number of non-zero components necessary to represent a signal on some basis. If y is measurement vector, x signal of interest and \emptyset sensing matrix, then the model-based compressive sensing can be expressed as:

$$y = \emptyset \cdot x \tag{1}$$

$$\begin{bmatrix} y_1 \\ \vdots \\ y_M \end{bmatrix} = [\emptyset_{M \times N}] \begin{bmatrix} x_1 \\ \vdots \\ x_N \end{bmatrix} \tag{2}$$

Note that $M \ll N$ resulting in an undetermined linear system.

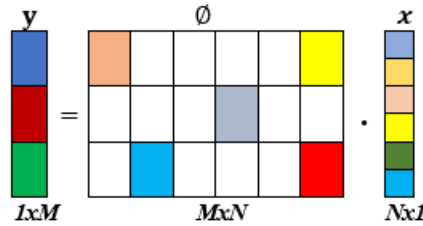


Fig. 1. Show that $M \ll N$ resulting in an undetermined linear system

For example, using maximum pooling under sampling techniques can be used to find \emptyset from origin data as shown below:

TABLE I. FIND \emptyset FROM ORIGIN DATA

2	4	1	3	By max pooling	8	3
6	8	2	1		9	5
9	1	5	1			
4	2	3	4			

Typical approach that usually can be used in the reconstruction technique is the Pseudo inverse, this leads to minimal \mathfrak{S}_2 solution.

$$x^{\wedge} = \emptyset^T (\emptyset \emptyset^T)^{-1} \cdot y \tag{3}$$

Note that, \mathfrak{S}_2 yields MMSE solution not sparsest solution, hence the solution; \mathfrak{S}_1 enforces sparsity. So employing the minimum on $\|x\|_{\mathfrak{S}_1}$ that subjected to $y = \emptyset \cdot x$ will solve the problem such that x is not inherently sparse. Now let ϕ represent a basis

upon which x is sparse. Then ϕ^{-1} is a linear operating mapping such that $x \rightarrow x^*$ where x^* is the projection onto basis ϕ will lead to:

$$x^* = \phi^{-1} x \tag{4}$$

$$y = \emptyset \phi x^* \tag{5}$$

This can be summarized by the following matrix notation given below:

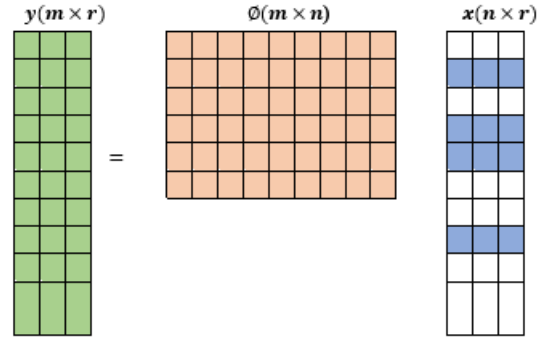


Fig. 2. The block diagram of an Image sparse using under sampling technique and Wavelet transformation

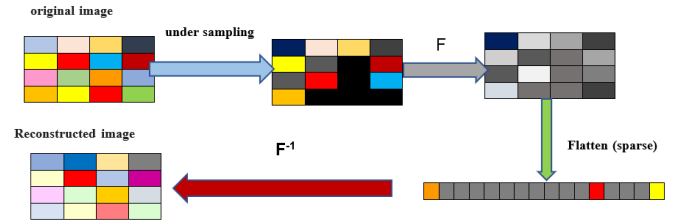


Fig. 3. Block diagram of image compressive sensing

III. THE PROPOSED METHOD

In the previous years, many classical chaotic systems were proposed, some of which depend on a pocket map, others that use a logistic map, and some adopt the idea of a tent map, etc. All of these systems are characterized by their simple mathematical forms, in addition to the well-known ease of implementation. Of course, it suffers during its performance from small key spaces and the possibility of detecting its orbits in addition to its limited ranges, and several other performance limitations. The authors proposed a high-dimensional chaotic system and the possibility of more secure encryption when used in image encryption and named it Walid-Ali Chaotic Map (WAM) [26-30]. Based on these characteristics, this new chaotic system (WAM) has been used in this research to generate chaotic sequences, which can be described by the following equations:

$$X_{n+1} = 1 - a X_n Y_n - X_{n2} - Y_{n2} - b \sin(Z_{n2}) \tag{6}$$

$$Y_{n+1} = X_n \tag{7}$$

$$Z_{n+1} = \pi - Y_n - c \sin(Z_n) \tag{8}$$

Note that a, b, and c are the parameters of system control while x, y, and z are system variables. In this paper, image encryption could be divided into three phases namely the block compressive sensing, and the Walid-Ali Chaotic Map (WAM)

system is employed to generate chaotic matrices for encryption processes. As well as, the block partition and Signature pseudo random sequence generator is implemented on the natural image. Finally, RSPD concept is used for encoding and decoding.

The main block diagram of the proposed method is given in Fig. 2. It can be divided into two main parts, namely the proposed block compression and Nharain chaos [17] encryption. The detail processing of the input image is described through the following demonstrated example of a given matrix.

Step 1:

- Given a natural image Y of size N*N usually N=512.
- Group the natural image into eight bits each hence H=[h1...h64] is formed and a total of 64 groups are formed of hexadecimal.
- Compute the following parameters (m1, m2, m3, m4, m5) using the following equations.

$$m1=h1\oplus h5\oplus h9\oplus \dots\oplus h61$$

$$m2=h2\oplus h6\oplus h10\oplus \dots\oplus h62$$

$$m3=h3\oplus h7\oplus h11\oplus \dots\oplus h63$$

$$m4=h4\oplus h8\oplus h12\oplus \dots\oplus h64$$

$$m5=h1+h3+h5+\dots+h6$$

$$m6=h2+h4+h6+\dots+h64$$

For simplicity we will take only sixteen decimal values as shown in the matrix bellow 4 by 4 elements hence the values of m1 up to m6 will be as computed bellow. Hence, the decimal values for this special case h1 ... h16

TABLE II. THE MATRIX BELLOW 4 BY 4 ELEMENTS

66	56	67	8
56	85	36	34
45	76	56	42
56	67	36	56

$$m1=66 \text{ xor } 56 \text{ xor } 67 \text{ xor } 8 = 49, m2=56 \text{ xor } 85 \text{ xor } 36 \text{ xor } 34 = 107$$

$$m3=45 \text{ xor } 76 \text{ xor } 56 \text{ xor } 42 = 115, m4=56 \text{ xor } 67 \text{ xor } 36 \text{ xor } 56 = 103$$

$$m5= 66 + 56 + 67 + 8 = 197 \quad \text{and} \quad m6= 56 + 85 + 36 + 34 = 211$$

- Compute four values namely A, B, C and D using the following equations.

$$A = \frac{m1 + m2}{256} + \frac{m5}{m3}, B = \frac{m3 + m4}{256} + \frac{m6}{m2}, C = \frac{m1 + m3}{256} + \frac{m5}{m4} \quad \& \quad D = \frac{m2 + m3}{256} + \frac{m6}{m1}$$

$$A = ((49+107)/256) + (197/115) = 2.3224$$

1+the following equation on bellow to get

$$B = ((115+103)/256) + (211/107) = 2.8235$$

$$C = ((49+115)/256) + (197/103) = 2.5532$$

$$D = ((107+115)/256) + (211/49) = 5.1733$$

- The initial values of random generated parameters (a1, a2, a3, a4, a5) can be obtained through the following equations and that will be as the keys through all the proceeding of the algorithm.

$$a1 = \frac{\text{mod}(A + B, 255)}{255}, a2 = \frac{\text{mod}(C + D, 255)}{255}, a3 = \frac{\text{mod}(A + B + C, 255)}{255}$$

$$a4 = \text{mod}(B + C + D, 1) \quad \& \quad a5 = \text{mod}(B + D, 3)$$

orithm. Thatat increasalgorithm.

$$a1 = \text{mod}(2.3224 + 2.8235, 255) / 255 = 0.0202, \quad a2 = \text{mod}(2.5532 + 5.1733, 255) / 255 = 0.0303,$$

$$a3 = \text{mod}(2.3224 + 2.8235 + 2.5532, 255) / 255 = 0.0302, \quad a4 = \text{mod}(2.8235 + 2.5532 + 5.1733, 1) = 0.5500$$

$$\& \quad a5 = \text{mod}(2.8235 + 5.1733, 3) = 1.9968$$

Step 2:

Compute the DWT in order to produce the sparse of the natural image P. here a Haar type is used of orthogonal matrix Ψ of dimension 4 * 4. Using the following equation:

$$P2 = \Psi * Y * \Psi^t \tag{9}$$

$$Y = [12 \ 15 \ 17 \ 4; 34 \ 76 \ 34 \ 23; 34 \ 6 \ 4 \ 22; 13 \ 5 \ 17 \ 18];$$

$$\Psi = [0.7071 \ 0.707 \ 0 \ 0; 0 \ 0 \ 0.707 \ 0.707; 0.707 \ -0.707 \ 0 \ 0; 0 \ 0 \ 0.707 \ -0.707]$$

$$P2 = [68.5 \ 39 \ -22.5 \ 12; 29 \ 30.5 \ 18 \ -9.5; -41.5 \ -18 \ 19.5 \ 1; 11 \ -4.5 \ 10 \ -8.5]$$

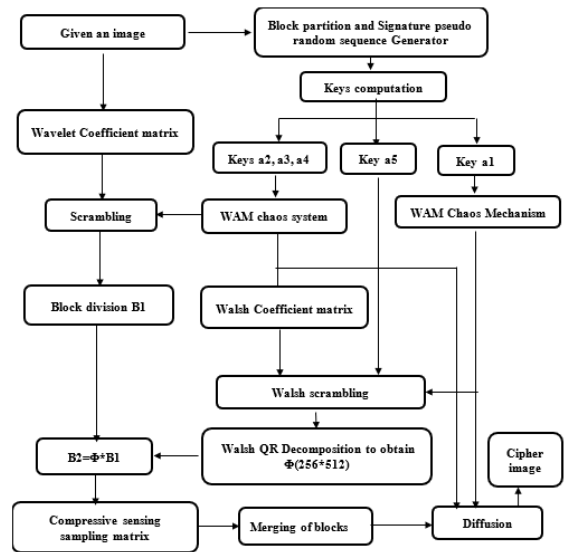


Fig. 4. The schematic diagram of the proposed compressed Encryption process

Step 3:

1-convert P2 into one dimensional vectors size m time's n to produce the vector P3

$$P2 = [68.5 \ 39 \ -22.5 \ 12 \ 29 \ 30.5 \ 18 \ -9.5 \ -41.5 \ -18 \ 19.5 \ 1 \ 11 \ -4.5 \ 10 \ -8.5]$$

2-scramble the element of P2 in step 2 above with the following expression:

$$P3(i) = P2(G(i))$$

G	2	6	7	9	1	3	5	1	1	1	8	4	1	1	1	1
=					5			6	0	3			1	4		2

$$P3 = [39 \ 30.5 \ 18 \ -41.5 \ 10 \ -22.5 \ 29 \ -8.5 \ -18 \ 11 \ -9.5 \ 12 \ 19.5 \ -4.5 \ 68.5 \ 1];$$

Step 4:

- Split the image into blocks B1 with dimension d*d and set compression ratio r=0.5, w=r*d for the current example d=4 and w=2.
- Using MM (measurement matrix) with the size 4*4 with Walsh transform.
- Generate three sequences of length n namely p, q and t by using Nharain logistic map.

$$K_{n+1} = k_n * r * (1 - k_n)$$

$$q = [0.20 \ 0.30 \ 0.10 \ 0.40], p = [0.30 \ 0.10 \ 0.40 \ 0.20] \text{ and } t = [0.40 \ 0.20 \ 0.30 \ 0.10]$$

- Quantized the values of the above sequences using the following equation.

$$f = \text{floor}(\text{mod}(k_n * 1015, N))$$

$$q = [2 \ 3 \ 1 \ 4], p = [3 \ 1 \ 4 \ 2] \text{ and } t = [4 \ 2 \ 3 \ 1]$$

- Scramble the sequences using Walsh transform depending on the value of the key a5. If a5 is 1 then shift the even rows of Walsh matrix to the left ti times and shift the odd rows to the right pi times. If a5=2 then shift the even rows of Walsh matrix to the right ti times and the odd rows to the left pi times. If a5=3 shift the even rows of Walsh matrix to the left ti times and shift odd rows to the right qi times.

$$a5 = 2$$

$$q = [2 \ 3 \ 1 \ 4]$$

$$p = [3 \ 1 \ 4 \ 2]$$

$$t = [4 \ 2 \ 3 \ 1]$$

1	1	1	1	1
1	-1	1	-1	1
1	1	-1	-1	1
1	-1	-1	1	1

1	1	1	1
-1	1	-1	1
-1	-1	1	1
1	-1	-1	1

- Finally the new Walsh matrix is rotated to clockwise 90 degrees to obtain the F matrix. Repeat shifting and rotation cycle 30 times to get the F2 matrix.

1	-1	-1	1
1	1	-1	-1
1	-1	1	-1
1	1	1	1

- In order to reduce the singular value of the MM a QR decomposition of F2 is computed. The Q is orthogonal and R is triangular.
- First F2t decomposed to matrix Q size n*m and matrix R size n*m upper triangular matrix and update the none diagonal element to zeros to get R1

$$Q = [-0.5 \ 0.5 \ 0.5 \ 0.5; -0.5 \ -0.5 \ 0.5 \ -0.5; -0.5 \ 0.5 \ -0.5 \ -0.5; -0.5 \ -0.5 \ 0.5 \ 0.5]$$

$$R = [-2 \ 0 \ 0 \ 0; 0 \ -2 \ 0 \ 0; 0 \ 0 \ -2 \ 0; 0 \ 0 \ 0 \ 2]$$

- Finally the MM Φ is synthesized by Qt and Rt.

$$Q_t = [-0.5 \ -0.5 \ -0.5 \ -0.5; 0.5 \ -0.5 \ 0.5 \ -0.5; 0.5 \ 0.5 \ -0.5 \ -0.5; 0.5 \ -0.5 \ 0.5 \ 0.5]$$

$$R_t = [-2 \ 0 \ 0 \ 0; 0 \ -2 \ 0 \ 0; 0 \ 0 \ -2 \ 0; 0 \ 0 \ 0 \ 2]$$

$$\Phi =$$

-0.5	-0.5	-0.5	-0.5	-2	0	0	0
0.5	-0.5	0.5	-0.5	0	-2	0	0
0.5	0.5	-0.5	-0.5	0	0	-2	0
0.5	-0.5	-0.5	0.5	0	0	0	2

Step 5:

Compress the block with the Φ
B2 = Φ*P3

$$\text{Block1} = -43.0000 \ 79.0000 \ -11.5000 \ -42.5000, \text{Block2} = -36.7500 \ -16.2500 \ -141.7500 \ -1.7500$$

Step 6:

- Reshape each block in to one vector and each vector is 1*4.

$$\text{Block1} = -43.0000 \ 79.0000 \ -11.5000 \ -42.5000$$

$$\text{Block2} = -36.7500 \ -16.2500 \ -141.7500 \ -1.7500$$

- Compute the quantification to each block to get the result decimal numbers range numbers between [0,255].

$$B3 = \text{round}\left[255 * \frac{B2 - \text{min}}{\text{max} - \text{min}}\right]$$

$$\text{Block1} = 114 \ 255 \ 150 \ 115$$

Block2= 121 145 0 162

- Reshape each block to w*d matrix blocks

Block1= 114 255 150 115

Block2= 121 145 0 162

Step 7: merge all blocks to the same location, the merged image is obtained of size w*n since w=r*m.

114 255 150 115

121 145 0 162

Step 8:

- Generate random number by the chaotic map

$x_{n+1} = x_n * r * (1 - x_n)$

$X_0 = a_1, X_1 = 0.0202 * 3.7 * (1 - 0.0202) = 0.0732, X_2 = 0.0732 * 3.7 * (1 - 0.0732) = 0.2510$

$X_3 = 0.2510 * 3.7 * (1 - 0.2510) = 0.6956, X_4 = 0.6956 * 3.7 * (1 - 0.6956) = 0.7834$

$X_5 = 0.7834 * 3.7 * (1 - 0.7834) = 0.6278, X_6 = 0.6278 * 3.7 * (1 - 0.6278) = 0.8646$

$X_7 = 0.8646 * 3.7 * (1 - 0.8646) = 0.4331, X_8 = 0.4331 * 3.7 * (1 - 0.4331) = 0.90$

- quantify the result of sequence number in the range [0 255] through the following equation.

$k = \text{floor}(\text{mod}(x * 1015, 255))$

$K_1 = \text{floor}(\text{mod}(0.0732 * 10^{15}, 255)) = 105, K_2 = \text{floor}(\text{mod}(0.2510 * 10^{15}, 255)) = 50$

$K_3 = \text{floor}(\text{mod}(0.6956 * 10^{15}, 255)) = 230, K_4 = \text{floor}(\text{mod}(0.7834 * 10^{15}, 255)) = 25$

$K_5 = \text{floor}(\text{mod}(0.6278 * 10^{15}, 255)) = 185, K_6 = \text{floor}(\text{mod}(0.8646 * 10^{15}, 255)) = 30$

$K_7 = \text{floor}(\text{mod}(0.4331 * 10^{15}, 255)) = 5, K_8 = \text{floor}(\text{mod}(0.9084 * 10^{15}, 255)) = 120$

x =	105	50	230	25	185	30	5	120
-----	-----	----	-----	----	-----	----	---	-----

Step 9:

- Compute the RSPD. Every pixel one the image is xor with the random number that have generated by logistic map one by one. The xor operations are computed from the first element to the end in the position of the sequence in the following equations.

$B_6(1) = x(1) \oplus B_5(1) \ \& \ B_6(i) = x(i) \oplus B_5(i) \oplus B_6(i-1)$

x =	105	50	230	25	185	30	5	120
-----	-----	----	-----	----	-----	----	---	-----

$B_6 = [27 \ 214 \ 166 \ 204 \ 12 \ 131 \ 134 \ 92].$

After that the first position is updated by the following equation:

$B_6(1) = B_6(m * N) \oplus B_6(1), B_6 = [71 \ 214 \ 166 \ 204 \ 12 \ 131 \ 134 \ 92]$

- By using the Z sequence random number that have generated by WAM chaos system used as index value for the B6 and produce new sequence and apply it with the following equation to obtain the B7 vector

$B_7(Z(1)) = x(m * N + 1) \oplus B_6(1) \oplus B_6(Z(1))$

$B_7(Z(i)) = x(m * N + i) \oplus B_6(Z(i)) \oplus B_6(Z(i-1))$

B6 =	71	214	166	204	12	131	134	92
Z =	3	1	4	6	8	5	2	7

X =	105	50	230	25	185	30	5	120
B7 =	41	5	114	253	30	25	120	185

Step 10: Finally, the cipher image with size m*N is obtained by the vector B7.

The flowchart of proposed compressed encryption system is given in Fig. 3.

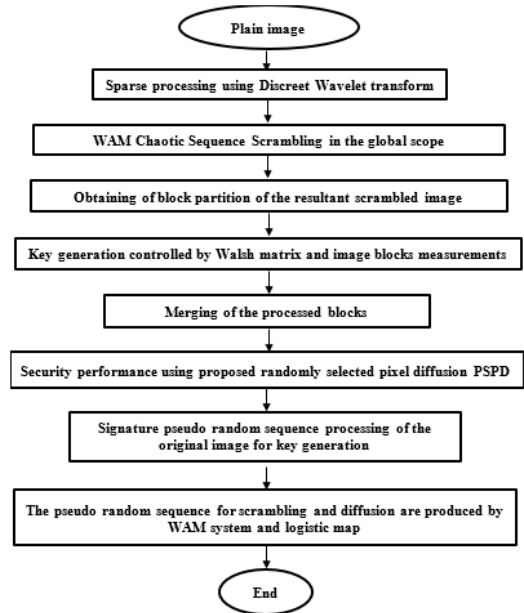


Fig. 5. The flow chart of the proposed compressed Encryption system

IV. EVALUATION OF THE PROPOSED ENCRYPTED SYSTEM

Multiple plain images database was selected in order to verify the performances of the proposed encryption system. Two main tests were carried out, namely, the compression capability and security performance. As well as the compression capability measured in order to achieve the accuracy required for the reconstruction process. In addition, the security capability was examine including the visual performance and secret key analysis, taking into account the conventional statistical,

differential, and malicious attacks. The result of comparisons of the proposed encryption system with several existing classical methods of showed that the proposed algorithm has smaller correlation coefficients compared with them.

TABLE III. COMPARES THE CORRELATION COEFFICIENTS OF THE PROPOSED METHOD TO THOSE OF OTHER METHODS

Encryption method	Vertical	Horizontal	Diagonal
Ref [23]	-0.0296	-0.0050	-0.0230
Ref [24]	0.00014	-0.00368	-0.02298
Ref [25]	0.0016	-0.0088	-0.0254
The proposed method	-0.0297	-0.0193	-0.0374

V. CONCLUSIONS

The main conclusions of this research are the following points: (1) the compression encryption model using BCS and WAM chaotic was implemented. (2) The diffusion mechanism and scrambling technique were designed, which succeeded in enhancement of secure performance. (3) Using of Walsh transform in the keys generation mechanism based on signature computation. (4) Testing results indicated that this proposed structure gives a low complexity and distinguished efficiency.

ACKNOWLEDGMENTS

The authors would like to thank the Iraqi Commission for Computer and Informatics, as well as the Informatics Institute for Post Grad, for their help and encouragement in performing this work.

REFERENCES

- [1] Kanso, A., & Ghebleh, M. (2015). An efficient and robust image encryption scheme for medical applications. *Communications in Nonlinear Science and Numerical Simulation*, 24(1-3), 98-116.
- [2] Banu S, A., & Amirtharajan, R. (2020). A robust medical image encryption in dual domain: chaos-DNA-IWT combined approach. *Medical & Biological Engineering & Computing*, 58, 1445-1458.
- [3] Hedayati, R., & Mostafavi, S. (2022). A lightweight image encryption algorithm for secure communications in multimedia Internet of Things. *Wireless Personal Communications*, 1-23.
- [4] Sang, Y., Sang, J., & Alam, M. S. (2022). Image encryption based on logistic chaotic systems and deep autoencoder. *Pattern Recognition Letters*, 153, 59-66.
- [5] Liu, H., & Wang, X. (2010). Color image encryption based on one-time keys and robust chaotic maps. *Computers & Mathematics with Applications*, 59(10), 3320-3327.
- [6] Hathot, S. F., Jubier, N. J., Hassani, R. H., & Salim, A. A. (2021). Physical and elastic properties of TeO₂-Gd₂O₃ glasses: Role of zinc oxide contents variation. *Optik*, 247, 167941.
- [7] Waheed, S. R., Suaib, N. M., Rahim, M. S. M., Adnan, M. M., & Salim, A. A. (2021, April). Deep learning algorithms-based object detection and localization revisited. *Journal of Physics: Conference Series* (Vol. 1892, No. 1, p. 012001). IOP Publishing.
- [8] Chai, X., Tian, Y., Gan, Z., Lu, Y., Wu, X. J., & Long, G. (2022). A robust compressed sensing image encryption algorithm based on GAN and CNN. *Journal of Modern Optics*, 69(2), 103-120.
- [9] Abdullah, A. H., Enayatifar, R., & Lee, M. (2012). A hybrid genetic algorithm and chaotic function model for image encryption. *AEU-International Journal of Electronics and Communications*, 66(10), 806-816.
- [10] Mansouri, A., & Wang, X. (2021). A novel one-dimensional chaotic map generator and its application in a new index representation-based image encryption scheme. *Information Sciences*, 563, 91-110.
- [11] Adnan, M. M., Rahim, M. S. M., Rehman, A., Mehmood, Z., Saba, T., & Naqvi, R. A. (2021). Automatic image annotation based on deep learning models: a systematic review and future challenges. *IEEE Access*, 9, 50253-50264.
- [12] Waheed, S. R., Rahim, M. S. M., Suaib, N. M., & Salim, A. A. (2023). CNN deep learning-based image to vector depiction. *Multimedia Tools and Applications*, 1-20.
- [13] Donoho, D. L. (2006). Compressed sensing. *IEEE Transactions on information theory*, 52(4), 1289-1306.
- [14] Tsaig, Y., & Donoho, D. L. (2006). Extensions of compressed sensing. *Signal processing*, 86(3), 549-571.
- [15] Waheed, S. R., Adnan, M. M., Suaib, N. M., & Rahim, M. S. M. (2020, April). Fuzzy logic controller for classroom air conditioner. *Journal of Physics: Conference Series* (Vol. 1484, No. 1, p. 012018). IOP Publishing.
- [16] Abdullah, H. A., Abdullah, H. N., & Mahmoud Al-Jawher, W. A. (2020). A hybrid chaotic map for communication security applications. *International Journal of Communication Systems*, 33(4), e4236.
- [17] Al-Helali, A. H. M., Mahmmoud, W. A., & Ali, H. A. (2012). A Fast personal palmprint authentication based on 3d-multi Wavelet Transformation. *International Journal of Scientific Knowledge*, 2(8).
- [18] Al-Jawher, W. A. (2007). New fast method for computing multiwavelet coefficients from 1D up to 3D. *Proc. 1st Int. Conference on Digital Comm. & Comp. App., Jordan* (pp. 412-422).
- [19] Salim, A. A., Ghoshal, S. K., & Bakhtiar, H. (2021). Tailored morphology, absorption and bactericidal traits of cinnamon nanocrystallites made via PLAL method: Role of altering laser fluence and solvent. *Optik*, 226, 165879.
- [20] Mahmoud, W. A., Abdulwahab, M. S., & Al-Taai, H. N. (2005). The determination of 3D multiwavelet transform.
- [21] Mahmoud, W. A. (2011). A smart single matrix realization of fast walidlet transform. *International Journal of Research and Reviews in Computer Science*, 2(1), 144.
- [22] Mahmoud, W. A., Hadi, A. S., & Jawad, T. M. (2012). Development of a 2-D wavelet transform based on kronecker product. *Al-Nahrain Journal of Science*, 15(4), 208-213.
- [23] Abdullah, H. A., Abdullah, H. N., & Mahmoud Al-Jawher, W. A. (2020). A hybrid chaotic map for communication security applications. *International Journal of Communication Systems*, 33(4), e4236.
- [24] Salim, A. A., Ghoshal, S. K., Bakhtiar, H., Krishnan, G., & Sapongi, H. H. J. (2020, April). Pulse laser ablated growth of Au-Ag nanocolloids: Basic insight on physiochemical attributes. *Journal of Physics: Conference Series* (Vol. 1484, No. 1, p. 012011). IOP Publishing.
- [25] Abbas, A. M., Abid, M. A., Abbas, K. N., Aziz, W. J., & Salim, A. A. (2021, April). Photocatalytic activity of Ag-ZnO nanocomposites integrated essential ginger oil fabricated by green synthesis method. *Journal of Physics: Conference Series* (Vol. 1892, No. 1, p. 012005). IOP Publishing.
- [26] Salim, A. A., Bakhtiar, H., Shamsudin, M. S., Aziz, M. S., Johari, A. R., & Ghoshal, S. K. (2022). Performance evaluation of rose bengal dye-decorated plasmonic gold nanoparticles-coated fiber-optic humidity sensor: A mechanism for improved sensing. *Sensors and Actuators: A. Physical*, 347, 113943.

- [27] Salim, A. A., Ghoshal, S. K., Shamsudin, M. S., Rosli, M. I., Aziz, M. S., Harun, S. W., ... & Bakhtiar, H. (2021). Absorption, fluorescence and sensing quality of Rose Bengal dye-encapsulated cinnamon nanoparticles. *Sensors and Actuators A: Physical*, 332, 113055.
- [28] Abdul-Kareem, A. A., & Al-Jawher, W. A. M. (2022). Uruk 4D discrete chaotic map for secure communication applications. *Journal Port Science Research*, 5(3), 131-142.
- [29] Salim, A. A., Bakhtiar, H., Bidin, N., & Ghoshal, S. K. (2018). Unique attributes of spherical cinnamon nanoparticles produced via PLAL technique: Synergy between methanol media and ablating laser wavelength. *Optical Materials*, 85, 100-105.
- [30] Kadhim, K. A., Najjar, F. H., Waad, A. A., Al-Kharsan, I. H., Khudhair, Z. N., & Salim, A. A. (2023). Leukemia Classification using a Convolutional Neural Network of AML Images. *Malaysian Journal of Fundamental and Applied Sciences*, 19(3), 306-312.
- [31] Waheed, S. R., Saadi, S. M., Rahim, M. S. M., Suaib, N. M., Najjar, F. H., Adnan, M. M., & Salim, A. A. (2023). Melanoma Skin Cancer Classification based on CNN Deep Learning Algorithms. *Malaysian Journal of Fundamental and Applied Sciences*, 19(3), 299-305.